

METEOROLOGICAL OFFICE

Boundary Layer Branch (Met O 14)

Turbulence and Diffusion Note No. 11

MEASUREMENTS OF ATMOSPHERIC TURBULENCE
DURING ATEX, FEBUARY 1969.

N Thompson

Note: As this paper has not been published, permission to quote from it should be obtained from the Head of the above Branch of the Meteorological Office.

MEASUREMENTS OF ATMOSPHERIC TURBULENCE DURING ATEX,
FEBRUARY 1969

By N Thompson

1. Introduction

ATEX (Atlantic Trade Wind Expedition) was a collaborative expedition involving (i) two German and one American Research ships at the corners of a triangle of side about 500 km and (ii) the Royal Navy Survey ship 'Hydra' sited at the centre of one of the sides of the triangle. All were making various meteorological and oceanographic measurements. The participation of Hydra provided the opportunity to test the prototype turbulence measuring system being developed for the Royal Society sponsored expeditions near OWS 'Juliet' which were then planned for 1970 and 1972. This note gives an outline of the system and an analysis of some of the data which were obtained.

2. Instrumentation

Measurements were made using equipment attached to the cable of a tethered kite balloon. The balloon was made specially for the purpose, and was thought to be the largest that could be conveniently handled from the flight deck of Hydra. It was a conventional design, 10 m long and 80 m³ volume with a free lift at the surface around 50 Kg. For safety reasons helium was used for inflation. The initial inflation was carried out under a net with ship headed into wind to give maximum shelter to the flight deck. Damage was most likely to occur on release or when being recovered for topping-up, in each case where the short length of tether could allow violent yawing motions of the balloon to occur. Fortunately these operations were carried out successfully, usually in winds of 7 to 10 m sec⁻¹. The balloon was otherwise kept at least 20 m above deck. The frequency of topping-up depended mainly on the amount of gas valved off during gain in altitude or as a result of solar radiation: the leakage through the fabric was negligible by comparison. A relatively strong (1000 Kg) tethering cable was used because of uncertainty about the extra stresses involved in flying a balloon from a moving platform, but it is now clear that 500 Kg cable can usually be used safely. 1000 Kg cable weighs about 5 Kg per 1000 m and its weight provides much of the limitation on maximum altitude. An electric winch with a very wide range of forward and reverse speeds was used to control the amount of cable paid out.

The turbulence package (shown diagrammatically in figure 1(a)) was designed to measure inclination (θ) of the wind to the horizontal using a hot-wire inclinometer, wind speed (V) in the vertical plane containing the wind vector by means of a photoelectric cup anemometer, and air and wet bulb temperatures (T and Tw) using fine platinum wire resistance thermometers: in the case of the wet bulb element the wire was twisted with cotton and wetted. The anemometer and inclinometer were based on a design by J I P Jones. A commercial radio telemetry system converted the various voltage outputs to frequencies which were then transmitted as a frequency multiplex via a simple dipole antenna. The ground equipment (figure 1(b)) included a phased crossed-dipole receiving antenna, radio receiver, magnetic tape recorder and a discriminator system consisting of band-pass filters and frequency-to-voltage converters, the outputs from which were displayed on a UV recorder. Downstream monitoring of the signal was used, that is the frequency multiplex was recorded on tape and monitored by the replay head of the tape recorder, only then being fed to the discriminators, thus providing a continuous check on tape recorder performance.

The radio system was delivered very late, only a few weeks before the expedition's start and a variety of problems were encountered with it, some of which were not properly resolved before the start. The main difficulty was caused by the voltage-controlled oscillators picking up high frequency signals from the transmitter: these signals appeared to be partly rectified within the oscillators and produced output frequency offsets comparable with the bandwidth of the oscillators. A variety of methods was used to attempt to filter out the unwanted signals but none was successful. Difficulties were also produced by lack of common-mode rejection by the VCO's, which was subsequently found to be due to the type of signal conditioning supplied by the manufacturer. This produced very large cross-talk between the temperature and wet-bulb channels: corrections have as far as possible been applied for this in the analysis described below (since ATEX a completely new signal conditioning system and technique of filtering have much improved the performance of the telemetry system (TDN 12)).

Occasionally the wet bulb was replaced by a sensitive differential pressure transducer which was used to measure vertical movement of the turbulent package: unfortunately it performed less well than expected, mainly because its satisfactory functioning necessitated a slight amount of balloon cable vibration, and this did not occur - this vibration is a feature of the balloon systems used at Cardington and presumably occurs there because of the higher cable tensions.

3. Synoptic conditions

The measurements were made a few degrees North of the Equator in a region of virtually continuous small-scale convection, limited by the trade-wind inversion which was always higher than the instrument package. The sea-air temperature difference was small, usually less than 1 degree C, but the near-surface moisture gradient was always significant with a typical mixing ratio change between surface and 10 m around 4×10^{-3} . The destabilising effect of this moisture gradient was thus equivalent to a temperature difference over the same height range of around 0.8 degree C so that significant instability was present even when the sea-air temperature difference was close to zero. Winds were usually between 7 and 12 metres per second. Showers were rare because of the limited height of convection.

4. Data and Data Processing

Nineteen experimental runs were made over periods ranging between about 40 minutes and 100 minutes. The instrument was usually flown at a fixed height between 50 and 400 m but in a few cases the observations were made successively at two different heights. Some of the data have been rejected because of instrumental difficulties with the probe, leaving twelve runs where at least V and ϕ were measured. Of these only five have been analysed so far (a fault developed on the band-pass filter card within the discriminator used to monitor the inclination signal and this meant that after run 6 it was impossible to monitor the inclination signal when the probe was airborne: the corresponding VCO had been tuned off-centre to allow for the effect of RF pickup but it now seems that an improper allowance was made for this in the later runs so that the actual transmitted frequency was outside the allocated bandwidth. Further attempts at filtering the signals are being made, at present without success).

Details of the experimental runs which were analysed appear in Table 1 together with relevant meteorological data. A sample of record from run 3 is shown in Figure 2: in this case the three signals were low-pass filtered to remove high frequency noise (and also some genuine fluctuations due to turbulence) and hence emphasise any peculiarities at lower frequencies. The filters were 4-stage

RC, with cut-off (- 12 db) at 5Hz. The most obvious features are large correlated fluctuations in wind speed and inclination with frequencies rather larger than 0.1 Hz which result from rise and fall of the ship and consequent relaxing and tightening of the balloon cable catenary. Also there are clearly significant variations with a frequency around 1 Hz; some preliminary spectral analyses of the data carried out at the Institute of Sound and Vibration Research at the University of Southampton using a high speed A-D converter interfaced directly with the computer showed the same results with a strong peak at 1 Hz undoubtedly due to noise and not turbulence. One cause of this is almost certainly bound up with the effects of RF pick-up mentioned earlier and probably comes about as follows. The balloon-borne turbulence 'package' actually consisted of two parts, a vane on which were mounted the sensors, and an electronics box about 1 metre below containing signal-conditioning circuits, batteries and the transmitter. Changes of relative orientation of vane and electronics box initiated perhaps by ship motion would often have been at the vane's natural frequency, which was about 1 Hz at the wind speeds which were found during ATEX. These changes in turn probably resulted in slight variations in the amount of RF pick-up by the VCO's and hence at least some of the observed noise. Periodic motions of the vane about its supporting axis (the balloon cable) would also have produced spurious signals due to displacement of the inclinometer pendulum from the true vertical. The other important features demonstrated by Figure 2 is the comparatively small size of the temperature fluctuations. This is typical of the marine atmosphere where the sea-air temperature differences are usually small.

An outline of the system used to digitise the data onto punched paper tape prior to data processing is shown in Figure 1 (c). The data on the magnetic tape were played back through the discriminators where automatic compensation for the effects of tape speed variation was applied and the resulting outputs were then low-pass filtered before digitisation by the Cardington low-speed data logger. Sampling details appear in Table 1. The sampling rate was 1 scan per second, with filter cut-off (- 3 db) at the Nyquist frequency.

The subsequent data analyses involved (a) reading data from the paper tapes to the KDF9 computer and conversion to meteorological parameters (V in $m\ sec^{-1}$, ϕ in degrees, T in degrees C and specific humidity) before writing to a KDF9 magnetic tape, (b) using these data to compute fluxes, standard deviations and vertical energy transports for various averaging times, and (c) computations of spectra and cross-spectra. Brief details of the relevant computer programmes appear in the Appendix.

5. Results

In principle the data are sufficient to determine in all cases the vertical momentum flux and spectra and cross-spectra, and except in run 2, the heat flux and temperature spectra also. However, due to cross-talk between the temperature and wet bulb depression channels in run 6 the heat flux data are unreliable in this instance: there are doubts too about the humidity data because the water supply to the wet bulb was incorrectly adjusted on this occasion and there are indications of the wet bulb element drying out.

In practice it is not possible to determine the various fluxes directly by the eddy correlation method because of the spurious correlations introduced by ship motion. Low-pass filtering with a suitable cut-off frequency will remove these spurious effects but will also attenuate some of the higher-frequency contributions to the fluxes. It is important therefore to be able to estimate the effective high-frequency limits of the co-spectra. McIlroy (1961) had insufficient data to draw any clear distinctions between momentum, heat and moisture transports: his results imply that high-frequency losses will be

negligible provided the cut-off frequency is less than about $2 \bar{U}/z$. Miyake et al (1970) also had limited data but were able to estimate separate limits for heat flux, and momentum and moisture flux. These were respectively $4\bar{U}/z$ and \bar{U}/z . At the lowest practical height of measurement (50 m) in a wind of 8 m sec^{-1} these latter correspond to cut-off frequencies around 0.6 and 0.2 Hz. The influence of ship motion on the measured fluxes therefore cannot be eliminated with certainty by low-pass filtering the data without attenuating the true fluxes, unless measurements are made several hundred metres above the surface. Nevertheless the raw flux calculations, ie those for different averaging times (Table 2), should provide at least a rough estimate if a suitable averaging time is chosen. Spurious contributions from ship motions are in the main at frequencies higher than about 0.1 Hz and so the relevant averaging times would be 8 or 16 seconds, equivalent cut-off being 0.06 and 0.03 Hz. A first inspection of the table shows that although the vertical momentum flux is downwards in every case as expected, there are substantial variations in magnitude between runs though the meteorological conditions appear to be virtually unchanging during the period over which these data were obtained. Some variation must of course result from the differing heights at which the data were obtained and possible ways in which this variation might be estimated are given later. The measured $\bar{U}w$ co-spectra show similar distortions in all five cases at their high frequency ends, presumably due to ship motion. Distortion amplitudes varied from run to run, perhaps because of varying height of measurement and state of sea; the worst case is shown in figure 3 (the curve drawn is an eye-fit of the data). Purely statistical variations in the co-spectral estimates are not large (each point represents a mean from 4 co-spectra in each of which the co-spectral estimates were averages across frequency of 8 raw estimates: the effective number of degrees of freedom is therefore 64, the number for a single unsmoothed estimate being 2. The corresponding variations for 80% confidence level are about $\pm 20\%$). The dip in the negative co-spectrum at around 2×10^{-2} Hz appears in all cases and may be a result of characteristic periodic excursions of the balloon acrosswind which would produce spurious $\bar{U}w$ correlation (Thompson 1969), though these seemed much less frequent than over land. It is encouraging to note that the main spurious correlations are all at frequencies higher than that giving values of $n z / \bar{U}$ around 1, the cut-off mentioned earlier. The net contribution to the measured flux can probably be assessed with sufficient accuracy by finding the area under the curve between about 9×10^{-2} Hz and the Nyquist frequency (referring now to Figure 3), after allowing for the fact that the eddy fluxes were calculated from filtered data whereas the co-spectral estimates are corrected for filter attenuation. This yields a value of $+0.535 \text{ dynes cm}^{-2}$ to be added to the flux calculated by eddy correlation from the raw (unaveraged) data, giving a corrected value of -0.74 ; a rough estimate for the effect of the dip at lower frequencies decreased this by about 5%. As one would expect this is close to the value calculated from the 8-second averaged data. Fluxes deduced in this way are given in Table 3. The scatter remains large and there is clearly no systematic variation with height. Errors due to the characteristic

TABLE 3

Momentum flux estimates (dynes cm^{-2})

Run Number	Height (m)	Raw estimate (no averaging)	Correction for $n > \bar{U}/z$	Correction for $n < \bar{U}/z$	Net corrected flux
2	180	- 0.369	+0.170	-0.008	-0.207
3	180	- 0.427	-0.408	-0.280	-1.115
4	90	- 0.111	-0.272	-0.072	-0.455
5	310	- 0.002	-0.532	-0.175	-0.709
6	90	- 1.275	+0.535	-0.038	-0.778

tethered balloon motion would be expected to amplify with height and so the relatively large measured flux in run 5 (310 m) may be much in error. It is worthwhile therefore considering further how the true flux might be expected to vary with height.

Assuming unaccelerated flow and a barotropic atmosphere, with the usual notation,

$$\frac{\partial \tau_{xz}}{\partial z} = \rho \beta (v_g - v) \quad (1)$$

$$\frac{\partial \tau_{yz}}{\partial z} = \rho \beta (u - u_g) \quad (2)$$

(here the x -axis is aligned along the mean wind direction at the surface). In the present experiments the momentum flux was calculated from $\rho \overline{U'w'}$ where U' refers to the instantaneous departure from the mean horizontal wind speed and thus the measured flux includes contributions from τ_{xz} and τ_{yz} . Over land, near the ground at least, results of Cramer et al quoted by Bernstein (1966) suggest that τ_{yz} is about an order less than τ_{xz} and that as a first approximation its contribution to the measured flux can be neglected. Pasquill and Tyldesley (1967) showed that

$$\overline{U'w'} \simeq \overline{u'w'} \left(1 + \frac{\overline{v'^2}}{2 \overline{u}^2} \right)$$

The magnitude of the momentum flux at any level assuming alignment of the x -axis along the mean wind direction is given by

$$\rho \sqrt{(\overline{u'w'}^2 + \overline{v'w'}^2)} \simeq \rho \overline{u'w'} \left(1 + \frac{\overline{v'w'}^2}{2 \overline{u'w'}^2} \right)$$

The error in approximating this by $\rho \overline{U'w'}$ is

$$\rho \overline{u'w'} \left(\frac{\overline{v'w'}^2}{2 \overline{u'w'}^2} - \frac{\overline{v'^2}}{2 \overline{u}^2} \right)$$

The latter term in the brackets is probably small over the sea because of the small surface roughness: the preceding term is apparently small near the surface as pointed out earlier but it may increase with increasing height. Swinbank's (1970) analysis of the 'Leipzig' profile, suggests that it remains small at all heights but a re-analysis of this profile by Carson (1971) shows an increase with height to significant values near the top of the boundary layer. However the ATEX data were obtained well below the top of the layer and so the measured momentum fluxes are likely to be close estimates of $\sqrt{(\tau_{xz}^2 + \tau_{yz}^2)}$.

During ATEX because of the persistent convection up to a marked inversion the boundary layer depth was not determined by surface roughness and geostrophic wind speed and so the variation of τ with height inferred by Carson from the Leipzig data is not relevant here. Typically the boundary layer depth was 1100 m (coincidentally equal to that for the Leipzig profile).

An approximation to the variation of τ close to the surface will be given by eq (1) which in this case may be written

$$\frac{\partial \tau_{xz}}{\partial z} = \rho \beta V_g \sin \alpha$$

where α is the angle between surface and geostrophic wind. Mendenhall (1967) determined average values for α over the sea after removing the effects of baroclinicity. He found the angle to increase with decreasing latitude but he had no data to extract its value at 11°N. At Johnson Island (17°N) it was around 10° in near neutral conditions - if a value of 15° is assumed relevant for ATEX then the variation of τ_{xz} with height is around 0.8×10^{-5} dynes cm^{-3} (V_g is assumed to be 9 m sec^{-1}). An estimate for τ at the surface can be obtained, probably within about 20% from

$$\tau_0 = \rho C_D \bar{u}_{10}^2$$

using a value of 1.3×10^{-3} for C_D (Brocks and Krugermeyer 1970). Taking \bar{u}_{10} as 8 m sec^{-1} gives $\tau_0 = 1.0 \text{ dynes cm}^{-2}$. Thus in the lowest 100 m apparently τ changes by 8%. This is a rate of decrease about half that inferred from the Leipzig profile by Carson and may be too low because α may have been underestimated (see below).

The above discussion has ignored baroclinicity: this may be included by re-writing eq (1) and (2) as:

$$\frac{\partial \tau_{xz}}{\partial z} = \rho \beta \left(v_g - v + \frac{z g}{\beta T} \cdot \frac{\partial T}{\partial x} \right) \quad (3)$$

$$\frac{\partial \tau_{yz}}{\partial z} = \rho \beta \left(u - u_g + \frac{z g}{\beta T} \cdot \frac{\partial T}{\partial y} \right) \quad (4)$$

where T is the surface temperature, provided the variation of T with height in the layer of interest, say the lowest 500 m, does not change significantly in the horizontal. The horizontal temperature gradient (from climatological charts) is $0.29^\circ\text{C}/100 \text{ Km}$ in the direction 187° . The resulting thermal wind is from 277° , increasing by $0.33 \text{ m sec}^{-1}/100 \text{ m}$. The surface geostrophic wind direction from climatological charts is 087° and the average surface wind direction during the 5 runs was 055° . The thermal and surface geostrophic winds are thus nearly opposed and the actual wind will begin to decrease with increasing height above the layer most influenced by surface friction, a familiar feature of the Trades (Charnock et al, 1956). The above data give α as 32° and $\partial \tau_{xz}/\partial z$ around 1.7×10^{-5} dynes cm^{-3} at the surface, a more reasonable value than the estimate above if one notes that $\tau_{xz} = 0$ where the ~~geostrophic~~ wind component along the x-axis begins to decrease with increasing height, at a height of a few hundred metres above the surface presumably. In the absence of any upper wind data (there were no wind-finding facilities aboard HYDRA) it is

difficult to provide any estimate for $\frac{\partial T_{uz}}{\partial z}$. It is non-zero at the surface and decreases as the geostrophic and actual wind approach one another. On any account it will make at least some contribution to τ . A comparatively large measured value for τ at 310 m is therefore plausible.

Some indication of the accuracy of the heat fluxes is given by results from run 5. Here a dummy temperature sensor (a metal-oxide resistor unshielded from radiation) was used and the calculated residual 'flux', approximated by that for 8-sec averaged data, was very small, about 0.2 mw cm^{-2} . Fluxes measured in the other runs using a proper temperature sensor were unfortunately also small, so presumably with comparatively large percentage error. They are at least consistent with the small measured sea-air temperature difference ($+ 0.3^\circ\text{C}$) which is in any case usually overestimated by a few tenths of a degree because the surface film is slightly cooler normally than water sampled by bucket (Hasse 1963). In the present cases the surface heat fluxes must therefore have been very close to zero. Because of the destabilising effect of the water-vapour gradient the density gradient was of course still unstable: latent heat carried up by moist 'thermals' would have been released in the upper part of the boundary layer and subsequently slowly transported downwards by predominant sinking motion between the organised upcurrents. The result would be a positive potential temperature gradient above the surface (often noted over land a few tens of metres above the surface on convective days, although then usually the result of transport of sensible heat by thermals to the upper boundary layer), and a downward heat flux at most heights which is consistent with the results of runs 3 and 4 (because of large cross-talk the heat flux estimated in run 6 must be discounted). The downward flux is probably a maximum around middle levels of the boundary layer and the observed flux change between 90 and 180 m is therefore realistic.

It was pointed out that the moisture data of run 6 are probably unreliable. On the other hand, using the flux values from the 8-sec averaged data as reasonable approximations to the actual fluxes at 90 m and the surface, and taking the 10 m wind as 8 m sec^{-1} leads to a value of 1.2×10^{-3} for k in the Jacobs formula often used to estimate evaporation:

$$E = (q_{\text{sea}} - q_{\text{air}}) e^k \bar{u}_{10}$$

this is to be compared with a similar value given by Robinson (1966), suggesting the moisture data may be more reliable than first thought.

In Table 4 the statistical data in the final columns of Table 2 have been combined with u^* to form non-dimensional standard deviations. The standard deviations have been approximated by those calculated from 8-second averaged data,

TABLE 4
Non-dimensional parameters

Run No	σ_{u/u^*}	σ_{w/u^*}
2	2.6	2.3
3	2.0	0.8
4	2.3	1.2
5	1.9	1.0
6	2.7	1.2
Averages	2.3	1.3

though this may lead to significant underestimations at the lower levels because spectra usually cover a higher frequency range than co-spectra so the appropriate cut-off frequency will then be higher than about \bar{U}/z . The scatter is large but the mean values are similar to estimates for the lower boundary layer (eg Lumley & Panofsky 1964) and this suggests the calculated momentum fluxes are realistic though of course \bar{u}_* itself is less sensitive to errors than τ .

6. Conclusions

While neither quality nor quantity of the data analysed is sufficient to provide a basis for firm conclusions there are nevertheless indications that some success was achieved in measuring fluxes of heat, moisture and momentum. In particular it seems possible to remove, without significantly affecting flux estimates, the spurious contributions due to ship motion. However there are indications of lower frequency tethered balloon motions producing spurious correlations in at least the Uw co-spectra over a frequency range where the co-spectral estimates would normally be expected to have appreciable relative magnitude.

APPENDIX

KDF 9 USERCODE PROGRAMMES TO PROCESS ATEX DATA

1. MPT08NT (Paper tape to magnetic tape conversion).

This will process any length of data written to paper tape in the order V, ϕ , T, T - T_w (the last two parameters are optional). If the data are the first set to be written to the magnetic tape (file 01), the programme will claim a 'blank' tape, title it, and then write selected data from a short constants tape as the next block. Thereafter, data are read from the paper tapes, converted from BCD to the appropriate parameters (m sec⁻¹, degrees, degrees C and specific humidity) and, after obviously faulty data have been detected and replaced by those immediately preceding, then written to magnetic tape as blocks, 512 numbers long. After all data are written further blocks are added which include a summary of the quantity of data in the file.

2. MPT06NT (Spectral and cross-spectral calculations).

This uses data on magnetic tape written by MPT08NT. The data are read to drum storage and U and w are computed after an axis rotation to make $\bar{w} = 0$. If the number of data for each channel are n, they are divided into lengths 1024 by forming n/1024, rounding up to give N and subdividing into lengths L = n/N. Linear trend corrections are applied to all these data lengths. Zeros are added to bring them to 1024 and Fourier coefficients calculated using an FFT routine written by R Rayment. Spectra and cross-spectra are then computed and the effects of analogue filtering and reduction of variance due to the adding of zeros are eliminated. The resulting spectral estimates are averaged across frequency in non-overlapping blocks of 8 to increase statistical significance before being output. Finally, means of the N individual spectra etc are also output. (It is expected that a graph plotting routine written by G H Jeffrey will be incorporated in the programme).

MPT07NT (Turbulent fluxes and variances for different averaging times).

This also uses data written to magnetic tape by MPT08NT. U and w are first computed, with an axis rotation to make $\bar{w} = 0$, and linear trend corrections are then applied. Data points are then averaged over overlapping lengths 2ⁿ (n = 0 to 7) and the quantities

$$\overline{e u'w'}, (\overline{c_p e T'w'}), (\overline{e q'w'}), \overline{u'^2}, \overline{w'^2}, (\overline{T'^2}), (\overline{q'^2}), \overline{w'u'^2}, \overline{w'^3},$$

$$(\overline{w'T'^2}), (\overline{w'q'^2})$$

are evaluated and output

for each averaging time.

REFERENCES

- Bernstein A B 1966 Examination of certain terms appearing in Reynolds' equations under unsteady conditions and their implications for micrometeorology, Q J R Met S, 92, No 394, pp 533-542.
- Brocks, K and Krugermeyer L 1970 The hydrodynamic roughness of the sea surface, Ber des Inst fur Rad und Mar Met, Univ Hamburg No 14
- Carson D J 1971 TDN (to be issued)
- Charnock H,
Francis J R D 1956 An investigation of wind structure in the Trades: Anegada 1953, Phil Trans Roy Soc A, 249, No 963 pp 179-234.
- and Sheppard P A
- Hasse L 1963 On the cooling of the sea surface by evaporation and heat exchange, Tellus, 15, pp 363-366
- Lumley, J L and
Panofsky H A 1964 The structure of atmospheric turbulence, Interscience publ.
- McIlroy, I C 1961 Effects of instrumental response on atmospheric flux measurements by the eddy correlation method. Div Met Phys Tech Pap No 11, CSIRO.
- Mendenhall B R 1967 A statistical study of frictional wind veering in the planetary boundary layer, Colorado State Univ., Atmos Sci Pap No 116.
- Miyake, M, Donelan M
and Mitsuta Y 1970 Airborne measurements of turbulent fluxes, J Geophys Res, 75, No 24, pp 4506-4518.
- Pasquill F and
Tyldesley J B 1967 TDN No 2
- Robinson G D R 1966 Another look at some problems of the air-sea interface, Q J R Met S., 92, No 394, pp 451-465
- Thompson N 1969 TDN No 5

TABLE 1 EXPERIMENTAL DETAILS

RUN NUMBER	DATE	TIME (Z)	PLACE	HEIGHT (M)	PARAMETERS MEASURED	MEAN SPEED (MSEC ⁻¹ (1))	SAMPLING RATE (SEC ⁻¹)	FILTER C/O (HZ)	SEA TEMP (DEG C)	AIR TEMP (DEG C)	WET BULB (DEG C)
2	6.2.69	1839 - 1947	11.0N 36.7W	180	U, ϕ	7.9	1.0	0.5	25.7	25.4	22.7
3	7.2.69	1300 - 1424	10.9N 37.1W	180	U, ϕ , T	9.1	1.0	0.5	25.4	25.2	22.5
4	7.2.69	1657 - 1740	10.8N 37.2W	90	U, ϕ , T	8.5	1.0	0.5	25.7	25.5	22.7
5	7.2.69	1907 - 2006	10.8N 37.2W	310	(U, ϕ , T (Dummy Sensor)	8.2	1.0	0.5	25.7	25.5	22.8
6	8.2.69	1307 - 1406	10.7N 37.5W	90	U, ϕ , T, T-Tw	9.5	1.0	0.5	26.0	25.6	22.5

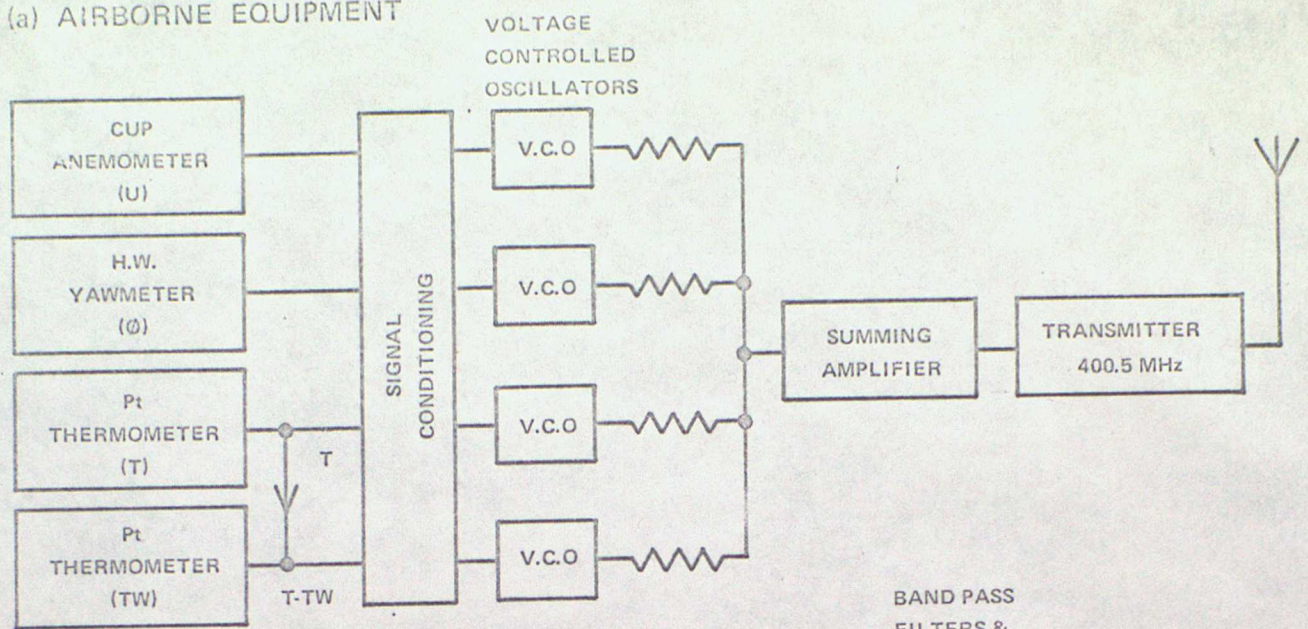
(1) Measured by turbulence probe and corrected for ship's wind-induced drift velocity

TABLE 2 FLUXES AND STANDARD DEVIATIONS

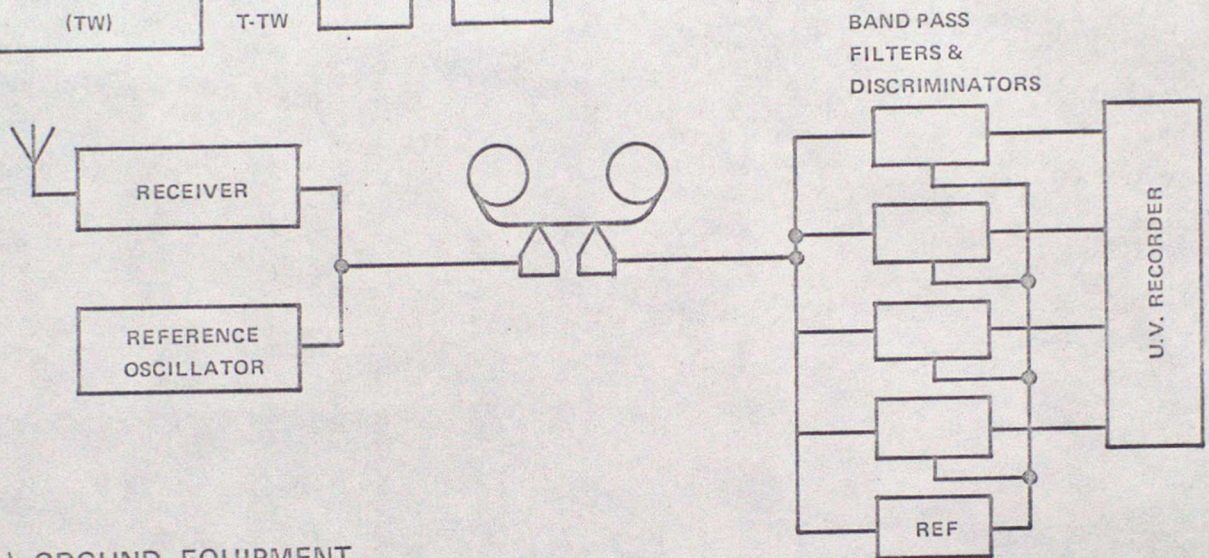
RUN NUMBER	AVERAGING TIME (SEC)	EQUIVALENT CUT-OFF FREQUENCY (HZ)	MOMENTUM FLUX (dynes cm ⁻²)	HEAT FLUX (mW cm ⁻²)	MOISTURE FLUX (g cm ⁻² sec ⁻¹)	σ_u (m sec ⁻¹)	σ_w (m sec ⁻¹)	σ_t (°C)	σ_q (g kg ⁻¹)
2 (180m)	-	-	-0.369			0.684	0.694		
	2	0.22	-0.243			0.610	0.606		
	4	0.11	-0.151			0.440	0.409		
	8	0.055	-0.191			0.348	0.303		
	16	0.027	-0.174			0.299	0.266		
	32	0.014	-0.164			0.254	0.236		
	64	0.007	-0.140			0.207	0.207		
	128	0.0035	-0.099			0.156	0.167		
3 (180m)	-	-	-0.427	-0.72		0.751	0.623	0.086	
	2	0.22	-0.226	-0.75		0.718	0.531	0.083	
	4	0.11	-0.267	-0.81		0.658	0.352	0.081	
	8	0.055	-0.471	-0.85		0.622	0.256	0.078	
	16	0.027	-0.513	-0.85		0.598	0.220	0.075	
	32	0.014	-0.539	-0.79		0.581	0.197	0.071	
	64	0.007	-0.504	-0.71		0.562	0.178	0.067	
	128	0.0035	-0.407	-0.62		0.538	0.156	0.061	
4 (90m)	-	-	-0.111	-0.20		0.542	0.568	0.109	
	2	0.22	0.032	-0.16		0.516	0.461	0.098	
	4	0.11	-0.188	-0.20		0.480	0.325	0.090	
	8	0.055	-0.361	-0.27		0.449	0.243	0.083	
	16	0.027	-0.366	-0.27		0.424	0.207	0.078	
	32	0.014	-0.340	-0.26		0.395	0.176	0.072	
	64	0.007	-0.267	-0.26		0.360	0.152	0.067	
	128	0.0035	-0.166	-0.22		0.318	0.131	0.061	

	128	0.0035	-0.166	-0.22		0.318	0.131	0.061	
	-	-	-0.002	0.11		0.656	0.391	0.192	
5 (310m)	2	0.22	-0.087	0.15		0.591	0.357	0.137	
	4	0.11	-0.330	0.19		0.517	0.302	0.098	
	8	0.055	-0.505	0.21		0.465	0.258	0.070	
	16	0.027	-0.525	0.19		0.439	0.243	0.051	
	32	0.014	-0.573	0.20		0.414	0.229	0.038	
	64	0.007	-0.605	0.18		0.391	0.212	0.030	
	128	0.0035	-0.571	0.14		0.369	0.191	0.024	
6 (90m)	-	-	-1.275	0.15	6.63×10^{-6}	0.805	0.978	0.054	3.46×10^{-4}
	2	0.22	-0.931	0.13	6.47	0.773	0.840	0.050	3.43
	4	0.11	-0.636	0.10	6.00	0.719	0.525	0.045	3.39
	8	0.055	-0.726	0.08	5.49	0.700	0.319	0.041	3.34
	16	0.027	-0.680	0.07	5.11	0.680	0.260	0.037	3.26
	32	0.014	-0.633	0.05	4.58	0.663	0.222	0.033	3.15
	64	0.007	-0.538	0.04	3.88	0.644	0.188	0.030	3.00
	128	0.0035	-0.411	0.03	2.97	0.624	0.145	0.026	2.81

(a) AIRBORNE EQUIPMENT



(b) GROUND EQUIPMENT



(c) DIGITIZING

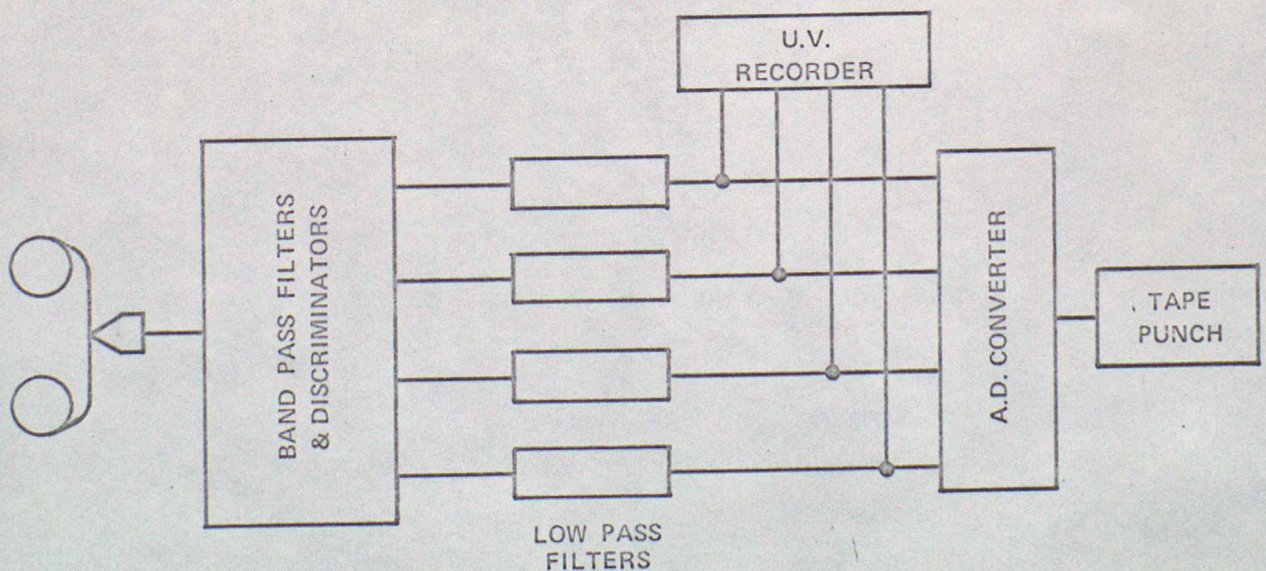


FIG 1. INSTRUMENTATION

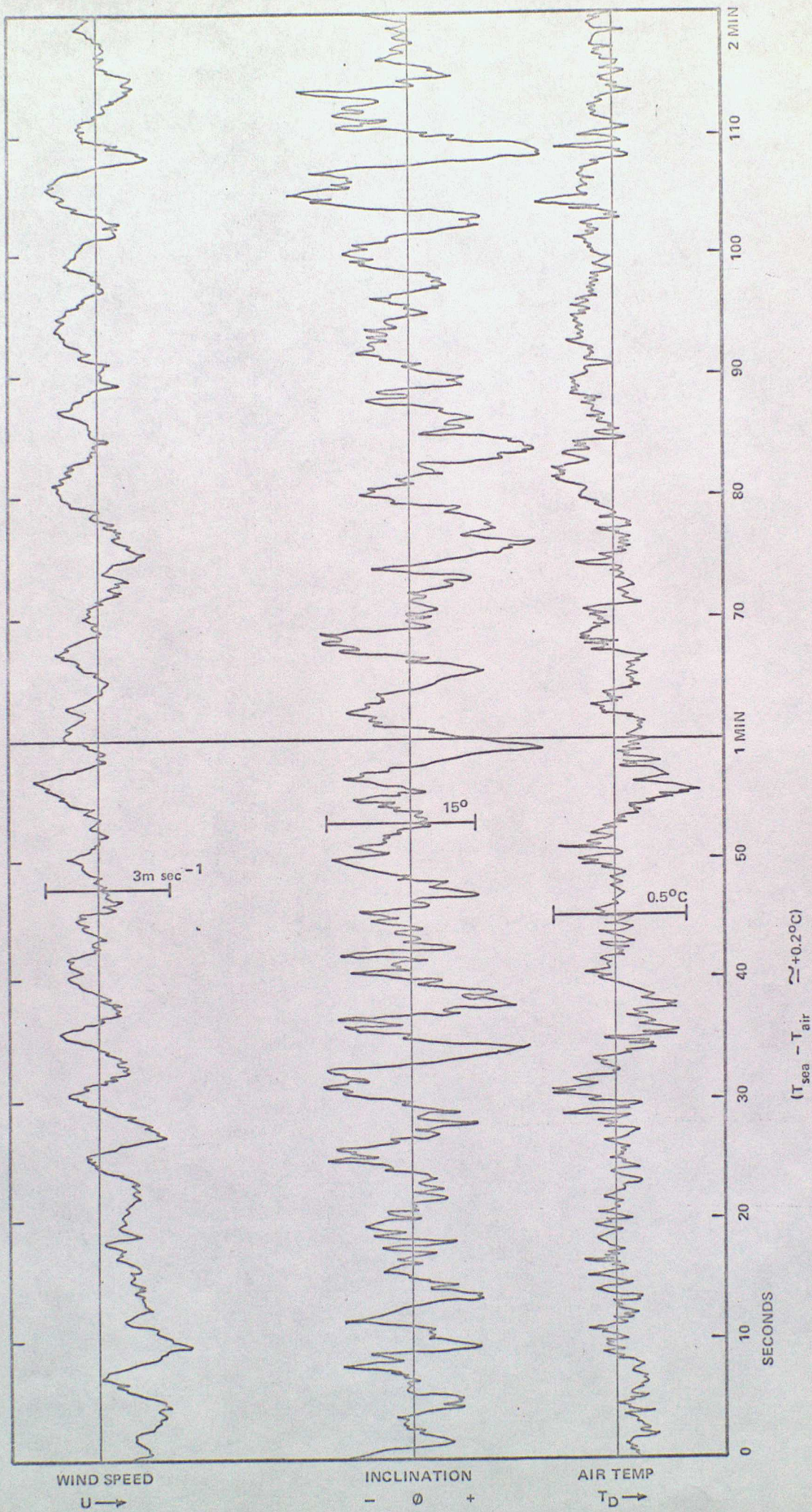


FIGURE 2 SIGNAL VARIATIONS DURING PART OF RUN 3

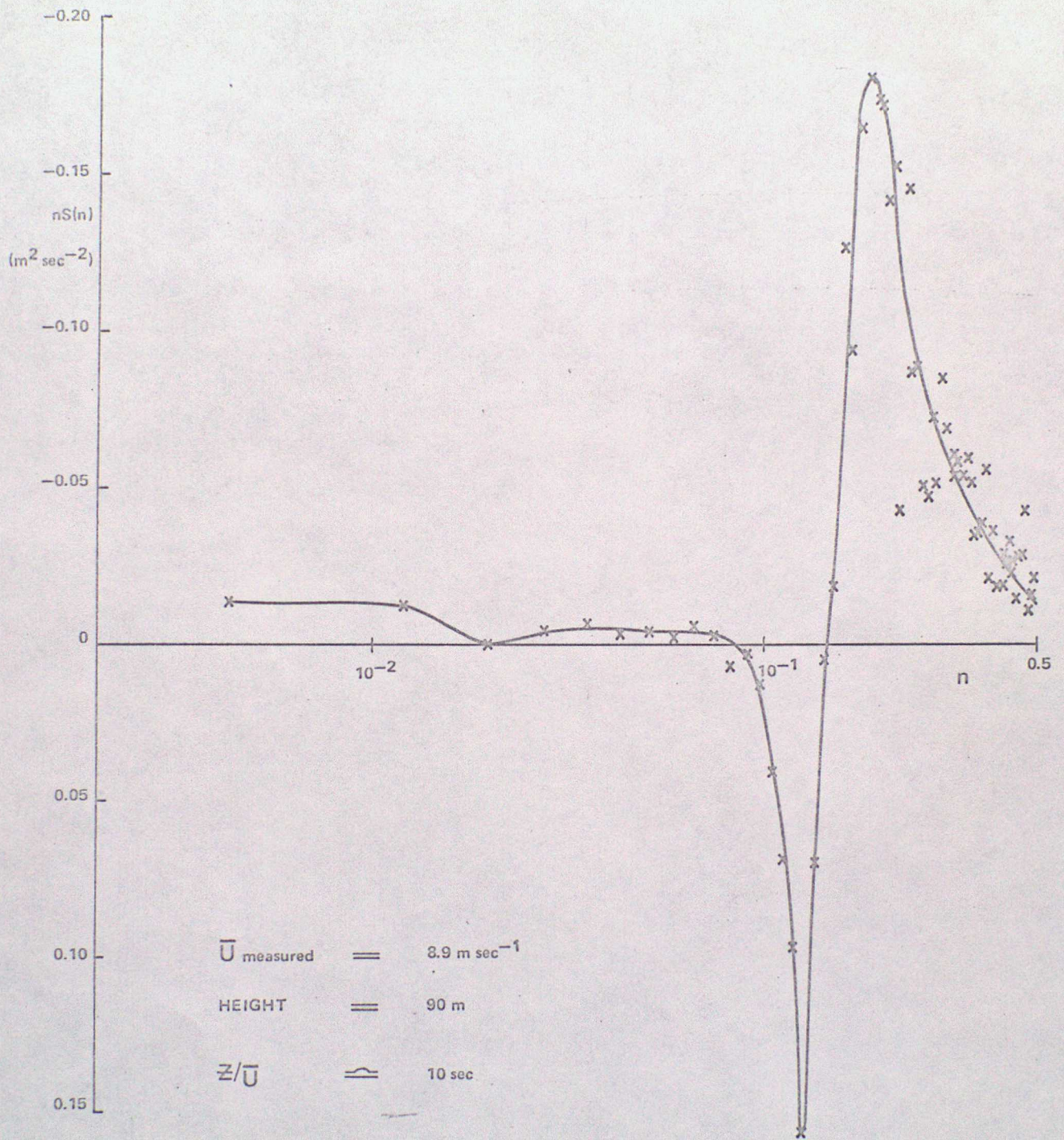


FIGURE 3 UW COSPEC, RUN 6